Brno University of Technology
Faculty of Mechanical Engineering
Energy Institute

Analysis of Two-Phase Flow Pattern Maps

Report: 16-09 / 14

Elaborated by: Noé Pinto del Corral

Revised:

Brno, September 2014

INDEX

1. Oshinowo-Charles's maps

1.1 Description of the map

Oshinowo-Charles (Oshinowo and Charles, 1974) suggested by experiment that the flow patterns depend on the volumetric flow rate of the gas flow and other fluid dynamic properties similar to the other maps. Therefore, the flow pattern can be estimated through Eqs. 1–3.

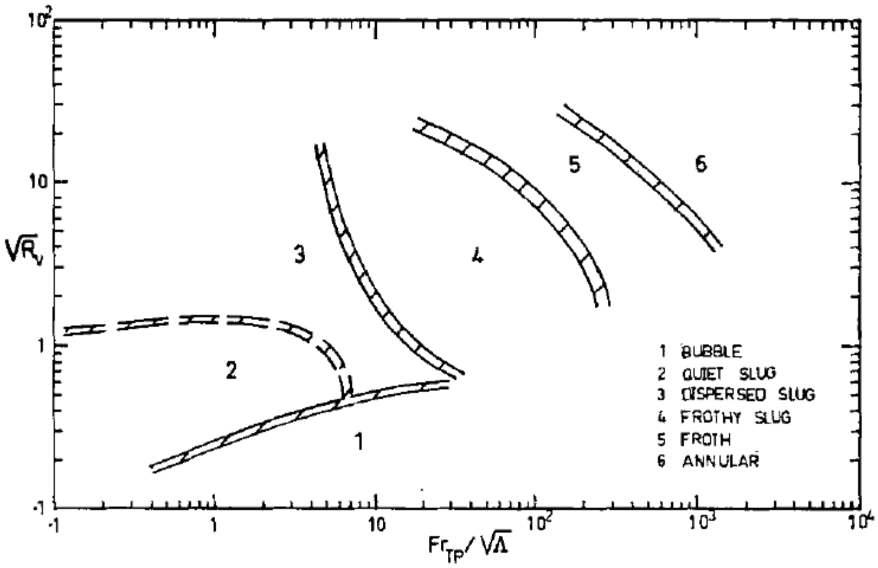

Figure 1.Oshinowo-Charles's map for up-flow vertical flux (Oshinowo and Charles, 1974).

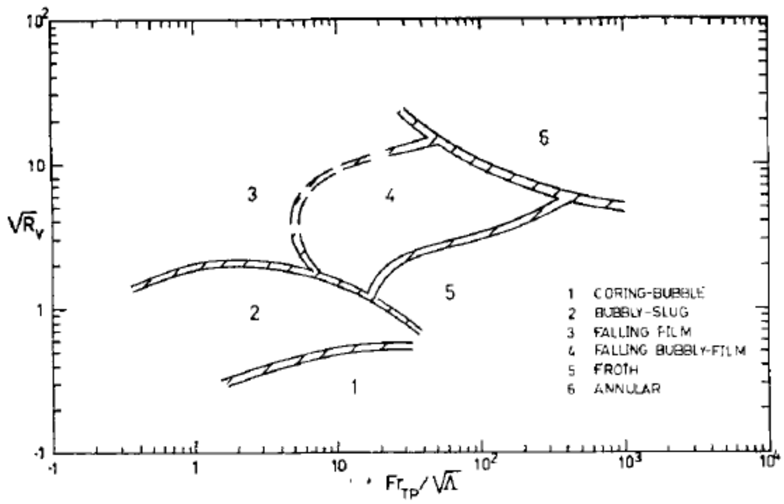

Figure 2.Oshinowo-Charles's map for down-flow vertical flux (Oshinowo and Charles, 1974).

$$R_v = \frac{Q_G}{Q_L} = \frac{u_G}{u_L} \qquad [-] \qquad (1)$$

$$F_{rTP} = \frac{(u_G+u_L)^2}{g \cdot D} \qquad [-] \qquad (2)$$

$$\Lambda = \frac{\mu_L}{\mu_W}\left[\frac{\rho_L}{\rho_W}\left(\frac{\sigma_L}{\sigma_W}\right)^3\right]^{-1/4} \qquad [-] \qquad (3)$$

Q_G is the volumetric flow rate of the gas, Q_L is the volumetric flow rate of the liquid, F_{rTP} is the Froude number of the two phases, u_g and u_l are the gas and liquid superficial velocities respectively.

1.2. Properties of the experiment. Limitations of the map

*Properties of the pipe:

-Length: 5.273 m

-Diameter: 2.54 cm

*Pressure: 0.71 barg

*Volumetric flux range for gas: 0 – $6.7 \cdot 10^5$ kg/m³h

*Volumetric flux range for liquid: $1.35 \cdot 10^5 - 2.4 \cdot 10^7$ kg/m³h

*Gas flow rate range: 1 – 104 kg/h

*Liquid flow rate range: 19 – 3540 kg/h

*Liquid density range: 1000 – 1250 kg/m³

*Liquid viscosity range (water–glycerin solutions): $1 \cdot 10^{-3} - 12 \cdot 10^{-3}$ kg/m s

*Surface tension: $68 \cdot 10^{-3} - 73 \cdot 10^{-3}$ kg/s²

*Temperature range: 10 – 27 °C

These were the conditions on which the experiment was done, but the authors have tested the *up-flow* map also with other data (from other authors), so maybe we could assume that the map is also valid for the following conditions (Oshinowo and Charles, 1974):

PUBLISHED DATA USED FOR TESTING THE GENERAL APPLICABILITY OF UPFLOW PATTERN REGIME MAP

System in Upflow	Pressure *atm.*	d_o in.	μ_L *cp.*	S_L	σ^* dynes/cm	Physical Property Parameter, $\Lambda^{1/2}$	Source
Steam-water	4.4	1.049	0.186	0.920	49.5	0.46	Runge[39]
	9.2	1.049	.0158	0.893	44.0	0.44	"
	14.6	1.049	0.141	0.870	40.0	0.44	"
	1.0	0.872	0.306	0.960	58.9	0.60	Isbin et al[20]
	21. ~ 81.	2.34	0.306	0.960	58.9	0.60	Schwartz[44]
Air-Heptane	1.0	0.50 1.03	0.42	0.684	22.0	1.05	Turner[48]
Gas-Heavy Oil	48.6**	3.00	18.0	0.85	26.5	6.24	Orkiszewski[29]
Air-Water	1.7 ~ 3.3	3.25	1.0	1.0	72.7	1.0	Rhodes[40]
	1.0	0.50 0.75 1.00	1.0	1.0	72.7	1.0	Griffith and Wallis[17]
	2.45	1.025	1.0	1.0	72.7	1.0	Govier et al[15]
Nitrogen-Mercury	1.3 ~ 2.9	1.049	1.55	13.6	490.0	0.45	Neal[26]
	1. ~ 2.***	2.0	1.55	13.6	487.0	0.45	Smissaert[42]

*Surface tension of water against steam obtained by extrapolation of data from references[19,52].
**This is the wellhead pressure. Measured pressure drop was 54.5 atm.
***Test channel was nickel-coated to promote mercury-wetted surface.

Table 1. Possible applications of Oshinowo and Charles's up-flow map (Oshinowo and Charles, 1974).

2. Hewitt and Roberts's map

2.1 Description of the map

The Hewitt and Roberts's map (Hewitt and Roberts's, 1969) is reasonably good for all water/air and water/steam systems over a range of pressures in small diameter pipes. The original map was created with British units, as we can see in the figure 3, but several authors have changed the units (e.g. Whalley, 1987).

Note: there is an error in the precision of the coordinate calculation in the original paper (Hewitt and Roberts, 1969). It causes uncertainties near the regime boundaries.

Carey pattern map for vertical flow is the same (or very similar) to the Hewitt and Roberts's map, so the limitations, properties etc. are all the same.

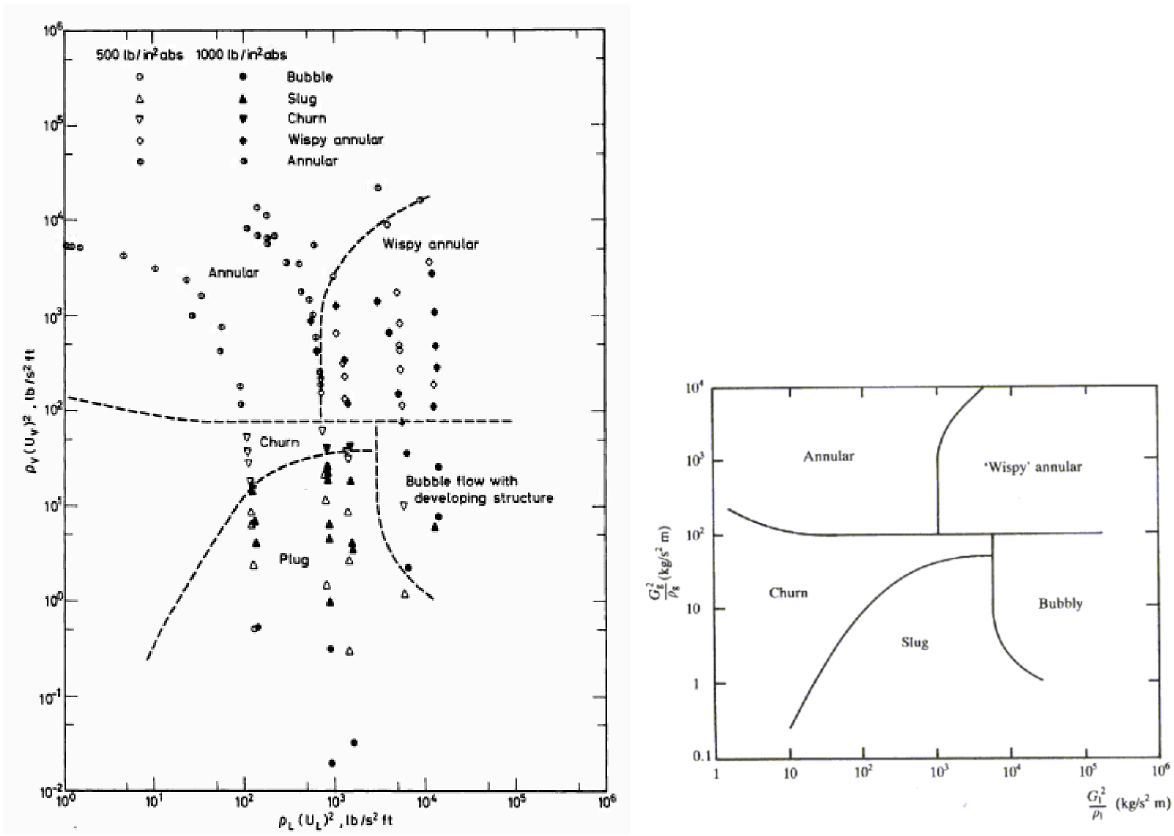

Figure 3. Hewitt and Roberts's map for vertical up-flow. At the left side, the original one (Hewitt and Roberts, 1969). At the right side, the map with SI units (Whalley, 1987).

2.2. Properties of the experiment. Limitations of the map

*Properties of the pipe:

-Length: 0.3 m

-Diameter: 31.75 mm

*Range of pressures at the mixing zone:

- Absolute pressure: $14.27 \cdot 10^4$ Pa – $54.26 \cdot 10^4$ Pa

- Relative pressure (P_0 – Patm): $4.14 \cdot 10^4$ Pa – $44.13 \cdot 10^4$ Pa

There also some experiments at higher pressures (500 and 1000 psig), showed in figure 3.

*Range of temperatures:

- Temperature of the gas: 18.9°C – 25.3°C

- Temperature of the liquid: 20.8°C – 32.5°C

*Flow rates range:

- Gas: 1.36 kg/h – 544.3 kg/h

- Liquid: 226.8 kg/h – 8164.7 kg/h

*Properties of the substances (Basically they consist in water/air or water/steam systems):

-Gas density range: 1.68 kg/m^3 – 6.4 kg/m^3

-Liquid density range: 992.2 kg/m^3 – 997.8 kg/m^3

3. Taitel and Dukler's map

3.1 Description of the map

The Taitel and Dukler's (1976) map (Taitel and Dukler, 1976) is the most widely used flow pattern map for horizontal two-phase flow. This map is based on a semi-theoretical method, and it is computationally more difficult to use than other flow maps. The horizontal coordinate of the Taitel and Dukler's (1976) map is the Lockhart–Martinelli parameter (Lockhart and Martinelli, 1949). The vertical coordinates of the Taitel and Dukler's (1976) map are K on the left hand side and T or F on the right hand side. They are defined as follows:

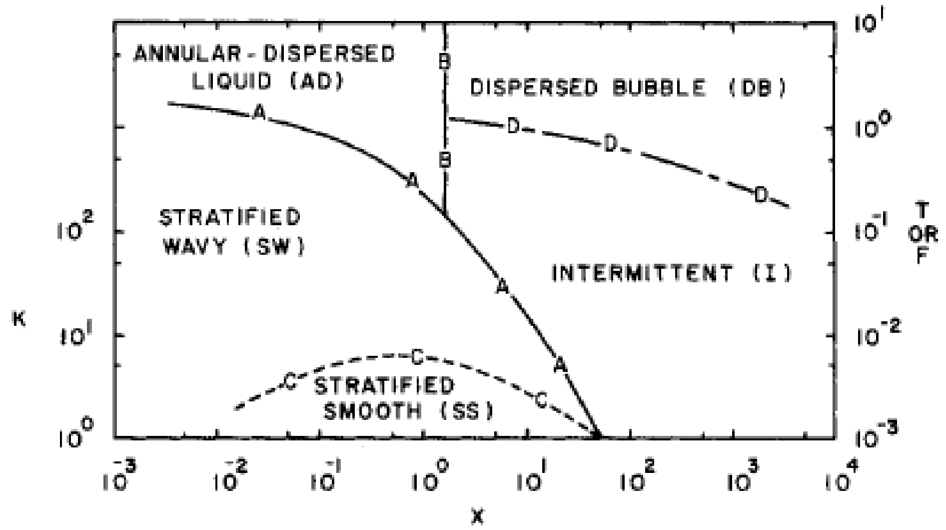

Figure 4. Taitel and Dukler's map for horizontal tubes (Taitel and Dukler, 1976).

$$X = \left[\frac{\frac{4C_L}{D}\left(\frac{u_{Ls}D}{\nu_L}\right)^{-n}\frac{\rho_L (u_{Ls})^2}{2}}{\frac{4C_G}{D}\left(\frac{u_{Gs}D}{\nu_G}\right)^{-m}\frac{\rho_G (u_{Gs})^2}{2}}\right]^{1/2} = \left[\frac{|(dP/dx)_{Ls}|}{|(dP/dx)_{Gs}|}\right]^{1/2} \quad [-] \qquad (4)$$

$$F = \sqrt{\frac{\rho_G}{\rho_L - \rho_G}}\,\frac{u_{Gs}}{\sqrt{Dg\cos\alpha}} \quad [-] \qquad (5)$$

$$K = F\left[\frac{Du_{Ls}}{\nu_L}\right]^{1/2} = F[Re_{Ls}]^{1/2} \quad [-] \qquad (6)$$

The Lockhart–Martinelli parameter depends on the parameters C_L, C_G, n and m. The authors take the values of this parameters which correspond to turbulent gas and turbulent liquid flow, which is the case of greatest practical interest ($n = m = 0.2$, $C_G = C_L = 0.046$).

The authors use different coordinates for each transition boundary:

-Stratified to annular: X, F

-Stratified to intermittent: *X, F*
-Intermittent to dispersed bubble: *X, T*
-Stratified smooth to stratified wavy: *X, K*

3.2 Properties of the experiment. Limitations of the map

In principle, the map was developed using theoretical methods, so it should not have the restrictions of the experimental ones. Nevertheless, there have been taken some theoretical assumptions that could affect the accordance between some experiments and the Taitel and Dukler's map. Here we have some of these assumptions:

(a) The map was developed for Newtonian liquid–gas mixtures

(b) They assume that hydraulic gradient in the liquid is negligible at transition conditions.

(c) They use the Gazley criteria (Gazley, 1949) for smooth stratified flow (see Taitel and Dukler, 1976 for details)

(d) They use $n = m = 0.2$ and $C_G = C_L = 0.046$ which corresponds to turbulent gas and turbulent liquid.

(e) They use the following criteria for Stratified to Intermittent transition (see Taitel and Dukler, 1976, for details):

$$F^2 \left[\frac{1}{C_2^2} \frac{\tilde{u}_G \, d\tilde{A}_L / d\tilde{h}_L}{\tilde{A}_G} \right] \geq 1 \qquad (7)$$

where F is a Froude number modified by the density ratio:

$$F = \sqrt{\frac{\rho_G}{\rho_L - \rho_G}} \frac{u_G s}{\sqrt{Dg \cos\alpha}} \qquad [-] \qquad (8)$$

(f) They fix the transition between intermittent and Annular Dispersed in the following way:

$$\frac{h_L}{D} = 0.5 \ \rightarrow X = 1.6 \qquad [-] \qquad (9)$$

(g) Transition between stratified smooth and stratified wavy is given by:

$$K \geq \frac{2}{\sqrt{\tilde{u}_L} \, \tilde{u}_G \sqrt{s}} \qquad (10)$$

(h) Transition between intermittent and dispersed bubble is:

$$T^2 \geq \left[\frac{8\tilde{A}_G}{\tilde{S}_i {\tilde{u}_L}^2 (\tilde{u}_L \tilde{D}_L)^{-n}}\right] \qquad (11)$$

This map has been tested by the authors with the Mandhane et al. experimental data, showing a great accordance.

4. Digitized Shell's DEP 31.22.05.11 map

4.1 Description of the map

This map was created by the company Shell (Shell company, 2007), for transport (charge and discharge) of combustibles. The flow maps are generalized by using as parameters the gas and liquid Froude number respectively, based on the feed pipe velocity and diameter.

The gas and liquid Froude numbers are defined as follows:

-Gas Froude number

$$Fr_G = u_G \sqrt{\frac{\rho_G}{(\rho_L - \rho_G) g d_{fp}}} \quad [-] \qquad (12)$$

-Liquid Froude number

$$Fr_L = u_L \sqrt{\frac{\rho_L}{(\rho_L - \rho_G) g d_{fp}}} \quad [-] \qquad (13)$$

In the above formulae, u_g and u_l are the superficial gas and liquid velocity respectively in the feed pipe, and d_{fp} is the inner diameter of the feed pipe.

$$u_G = \frac{Q_G}{\left(\pi d_{fp}^2/4\right)} \quad [\mathrm{m/s}] \qquad (14)$$

$$u_L = \frac{Q_L}{\left(\pi d_{fp}^2/4\right)} \quad [\mathrm{m/s}] \qquad (15)$$

and the averaged liquid density ρ_L is defined as:

$$\rho_L = \frac{M_L}{Q_L} \quad [\mathrm{kg/m^3}] \qquad (16)$$

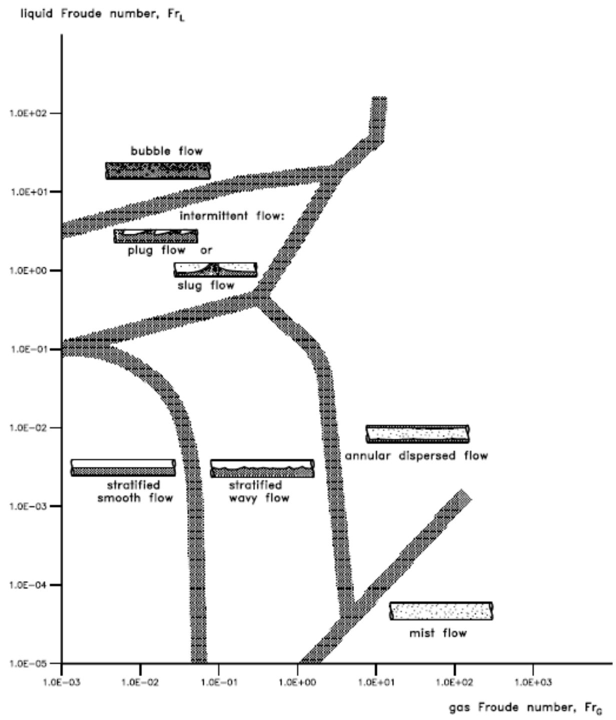

Figure 5. Shell's map for horizontal tubes (Shell company, 2007).

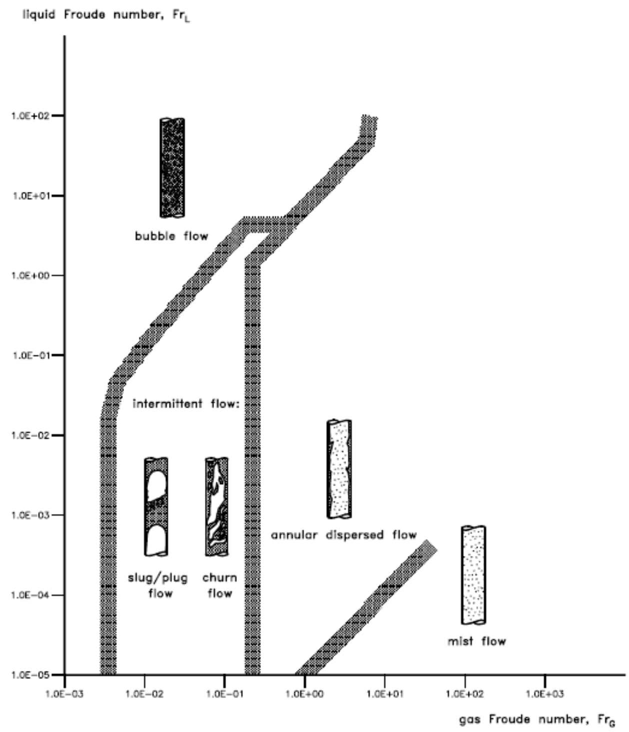

Figure 6. Shell's map for vertical tubes (Shell company, 2007).

4.2 Properties of the experiment. Limitations of the map

*Properties of the substances:

-Gas density: 8 kg/m³

-Liquid density: 860 kg/m³

-Gas viscosity: $1.2 \cdot 10^{-5}$ Pa s

-Liquid viscosity: $1.6 \cdot 10^{-4}$ Pa s

-Surface tension: 0.03 N/m

*Properties of the pipe:

-Diameter: 500 mm

As the maps are in these coordinates, and the conditions are the fixed characteristics given above, they vary the velocities, and one can suppose that they vary the fluxes or/and the pressures.

Anyway, with the conditions, we have: $F_{rG} = V_G \cdot \left(0.044\ \frac{\mathrm{s}}{\mathrm{m}}\right);\ F_{rL} = V_L \cdot (0.454\ \frac{\mathrm{s}}{\mathrm{m}})$

We can see at the figures that the Froude numbers vary from 10^{-5} to 10^{2} in the case of $F_{rL}$and 10^{-3} to 10^{2} in the case of F_{rG}. So, the velocities vary as:

V_L: $2{,}2 \cdot 10^{-5}$ – 220.3 m/s

V_G: 0,023 – $2.3 \cdot 10^{3}$ m/s

* In the same way, since the velocities depend on the flow rate, they seem to vary the flow rates as:

Q_L: $4.3 \cdot 10^{-6}$ – 43.2 $\mathrm{m^3/s}$

Q_G: $4.5 \cdot 10^{-3}$ – 450.8 $\mathrm{m^3/s}$

*They do not define any pressure in the while present the map, but one can read in their manual that they work in pressures below 90 bar ($\mathrm{P} < 9 \cdot 10^{6}$ Pa)

5. Griffith and Wallis's map

5.1 Description of the map

Griffith and Wallis's map (Griffith et al., 1959) was originally created for the study of slug flow in vertical direction. Therefore, the map shows the region in which the slug flow appears, but one cannot really trust in which the map says about the other patterns, since they do not have any experimental points in these areas (see Golan and Stenning, 1969).

The axes of this map were defined as follows:

Y axis: $\frac{Q_g}{Q_l+Q_g}$ [–]

X axis: $\left(\frac{Q_l+Q_g}{A_p}\right)^2 / gD_p$ [–]

Where, Q_g and Q_l are the gas and liquid volumetric flow rate respectively, A_p is the cross-section area of the pipe, D_p is the diameter of the pipe and g is the acceleration of gravity

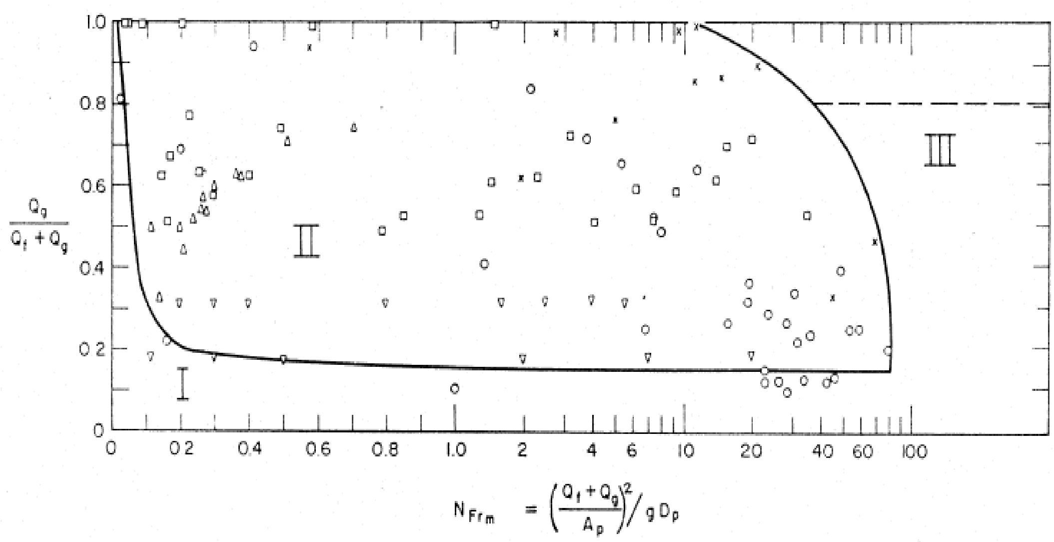

Figure 7: Griffith and Wallis's map (Griffith *et al.*, 1959).

5.2 Properties of the experiment. Limitations of the map.

*Liquid used: water

*Gas used: air

*Properties of the pipe:

-Length: 5.48 m

-Diameter: 1.27 – 2.54 cm

*Pressure: 1.013 barg

*Liquid density: 1000 kg/m^3

*Liquid viscosity: $1 \cdot 10^{-3}$ kg/m s

*Surface tension: $73 \cdot 10^{-3}$ kg/s^2

6. Golan and Stenning's map

6.1 Description of the map

Golan and Stenning (Golan and Stenning, 1969) found that there were some contradictions between the vertical flow maps created before theirs, and also saw that the Griffith and Wallis's map did not work so well. For these reasons, they made their own vertical map, both for up-flow and down-flow. The characteristics of both maps are the same; they simply use the superficial velocities as coordinates.

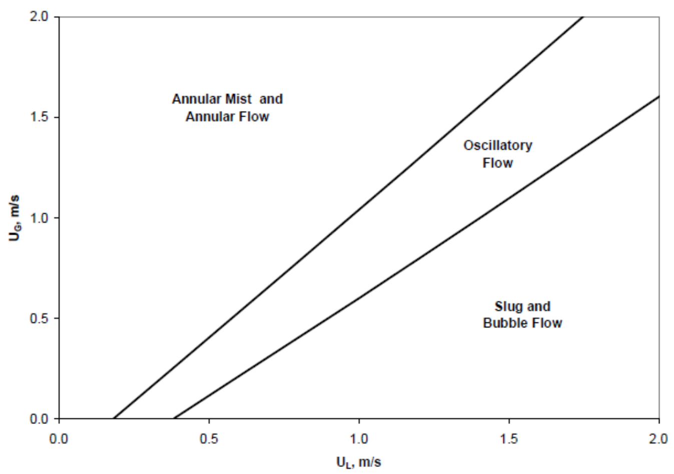

Figure 8: Golan and Stenning's map for down-flow in SI units (Pickering et al., 2001).

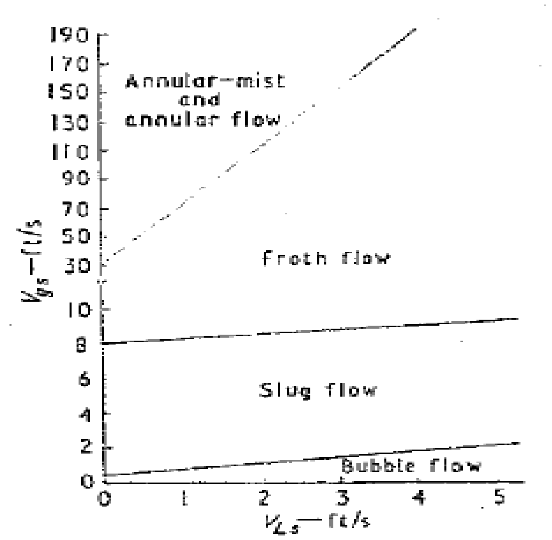

Figure 9: Golan and Stenning's map for up-flow (Golan and Stenning, 1969)

6.2 Properties of the experiment. Limitations of the map

*Liquid used: water

*Gas used: air

*Properties of the pipe:

- -Length: 3 m
- -Diameter: 3.81 cm

*Pressure: 3.12 barg

*Gas flow rate range: 10.77 – 3067.5 kg/h

*Liquid flow rate range: 1000 – 10000 kg/h

*Liquid density range: 1000 kg/m^3 (water)

*Liquid viscosity range: 10^{-3} kg/m s

*Surface tension: 0.072 kg/s^2

*Temperature range: 20°C

7. Mandhane-Gregory-Aziz's map

7.1 Description of the map

Mandhane et al. (Mandhane et al., 1974) realized that there were a lot of contradictions between the proposed maps until that moment, so they try to re-evaluate them with a very big amount of data. The used a data bank which has near 14000 experimental data from research results since 1962 until 1973 (AGA-API Two-Phase Flow Data Bank). They took all the results of horizontal flow and defined their own map.

Following their research, it seems that Baker's map (Baker, 1954) is not good enough, even if it is quite used in some industries.

Their final map is a kind of average of all experimental maps created until that moment, using 6000 experimental data points, and it seems to be better than the other ones on predicting the flow patterns.

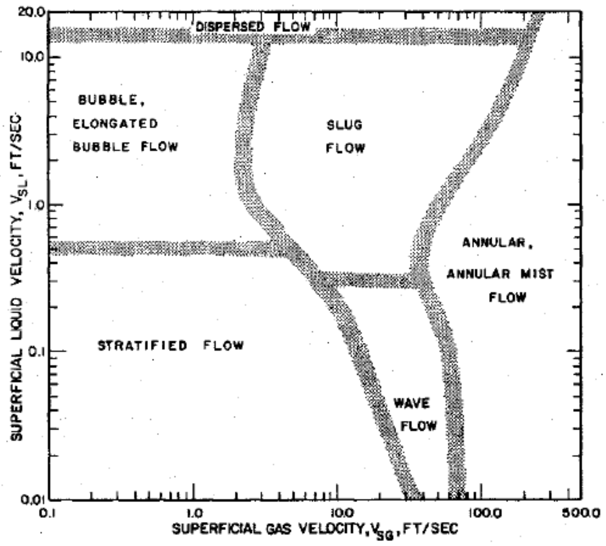

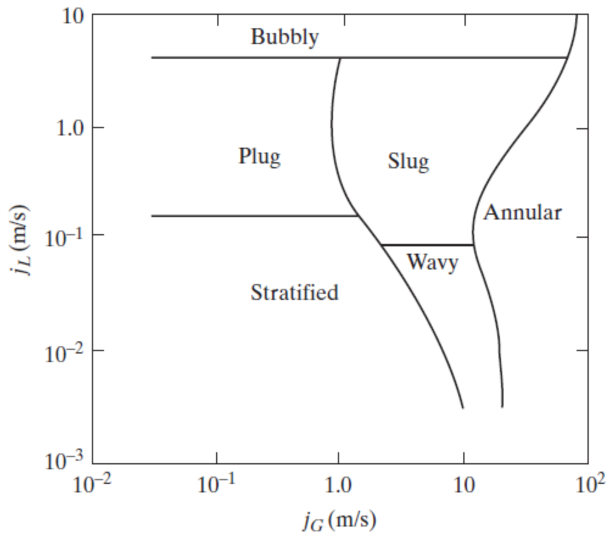

Figure 10: Mandhane-Gregory-Aziz's map for horizontal flow the upper one is the original (Mandhane et al., 1974), the second one is the same with SI units (Ghiaasiaan, 2008).

7.2 Properties of the experiment. Limitations of the map

In this case, there is not only one experiment, but one can read, in the Mandhane et al. paper, the ranges of some of the parameters that we need. The map works better for water-air systems and pipe diameters less than 5 cm. This is because most of the data that they took had these properties. Instead of that, the map works also well in the whole range defined below:

*Pipe diameter: 1.27 – 16.51 cm

*Gas flow rate range: $1.82 \cdot 10^{-5}$ – 730 kg/h *estimated*

*Liquid flow rate range: 0.054 – 632.5 kg/h *estimated*

*Liquid density range: 704.8 – 1009.2 kg/m^3

*Gas density range: 0.8 – 50.5 kg/m^3

*Liquid viscosity range: $3 \cdot 10^{-4}$ – 0.09 kg/m s

*Gas viscosity range: 10^{-5} – $2.2 \cdot 10^{-5}$ kg/m s

*Surface tension range: $24 \cdot 10^{-3}$ – 0.1 kg/s^2

*Superficial liquid velocity: $9 \cdot 10^{-4}$ – 7.32 m/s

*Superficial gas velocity: 0.043 – 170.7 m/s

8. Baker's map

8.1 Description of the map

The Baker's map (Baker, 1954) is one of the most used maps, even if it has some deficiencies pointed out by many authors (Bell et al., 1970; Mandhane et al., 1974 among others). It was generated by taking the data from Jenkins (Jenkins, 1947), Gazley (Gazley, 1949), Alves (Alves, 1953) and Kosterin (Kosterin, 1949). Baker used the λ and ψ parameters to take into account the properties of different gases and liquids. Figure 11 shows the original Baker's map, whose axes are defined as follows:

X-axis: $\frac{L\lambda\psi}{G}$ [–]

Y-axis: $\frac{G}{\lambda}$ [lb/h ft^2]

Where, L and G are the liquid mass flux and gas mass flux respectively

$$L = \frac{m_L}{S} \quad [\text{lb/h ft}^2] \qquad (17)$$

$$G = \frac{m_G}{S} \quad [\text{lb/h ft}^2] \qquad (18)$$

And λ and ψ parameters are defined as:

$$\lambda = \left[\frac{\rho_G}{\rho_{air}}\frac{\rho_L}{\rho_w}\right]^{1/2} \quad [–] \qquad (19)$$

$$\psi = \frac{\sigma_w}{\sigma_L}\left[\frac{\mu_L}{\mu_w}\left(\frac{\rho_w}{\rho_L}\right)^2\right]^{1/3} \quad [–] \qquad (20)$$

Where $\rho_{air} = 0.075\ \text{lb/ft}^3$ and $\rho_w = 62.3\ \text{lb/ft}^3$ are the densities of the air and water at room conditions, respectively, $\sigma_w = 73$ dyn/cm is the superficial tension of the water and $\mu_w = 1$ cp is the dynamic viscosity of water.

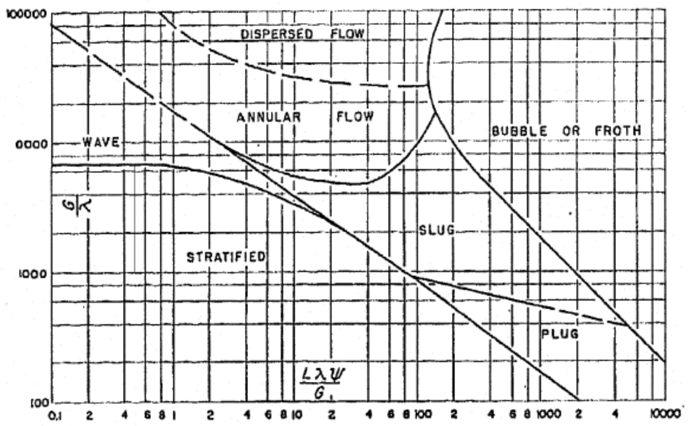

Figure 11: Original Baker's map for horizontal flow (Baker, 1954).

The original map from Baker was modified by Scott in 1964 (Scott, 1964), incorporating modifications to improve the agreement with the data of Hoogendoorn (Hoogendoorn, 1959) and of Govier and Omer (Govier and Omer, 1964), trying to include the effect of the pipe diameter. The modified map is shown in figure 12, and it corresponds to the "Modified Baker's map", the horizontal one, available in the website.

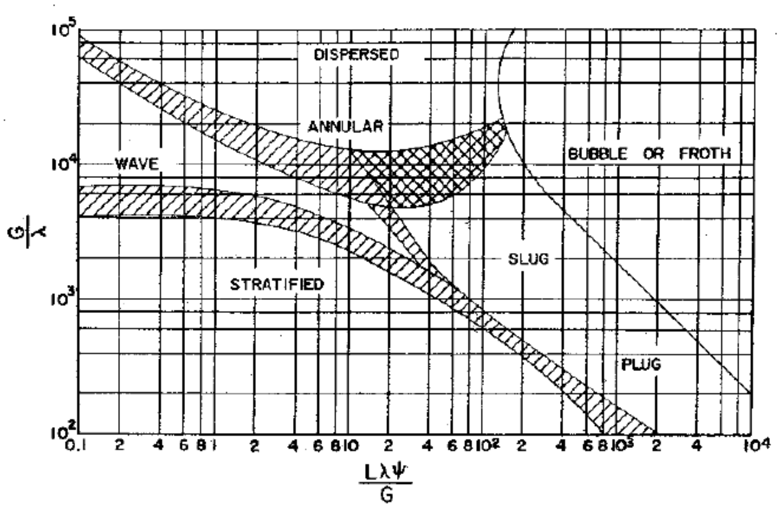

Figure 12: Modified Baker's map for horizontal flow (Scott, 1964).

Then, Bell et al. (Bell et al., 1970) made a redrawing of the original Baker's map by eliminating numerical constants from the axes (figure 13), redefining them as:

X-axis: $G_L\Psi$ [cm lb$^{2/3}$/dyne h$^{4/3}$ ft$^{1/3}$]

Y-axis: $\frac{G_v}{\Lambda}$ [ft/h]

Where,

$$G_L = L = \frac{m_L}{S} \quad [\text{lb/h ft}^2] \qquad (21)$$

$$G_v = G = \frac{m_G}{S} \quad [\text{lb/h ft}^2] \qquad (22)$$

$$\Psi = \frac{1}{\sigma_L}[\mu_L \rho_L^2]^{1/3} \quad [\text{cm ft}^{5/3}/\text{ dyne h}^{1/3}\text{ lb}^{1/3}] \qquad (23)$$

$$\Lambda = [\rho_L \rho_G]^{1/2} \quad [\text{lb/ft}^3] \qquad (24)$$

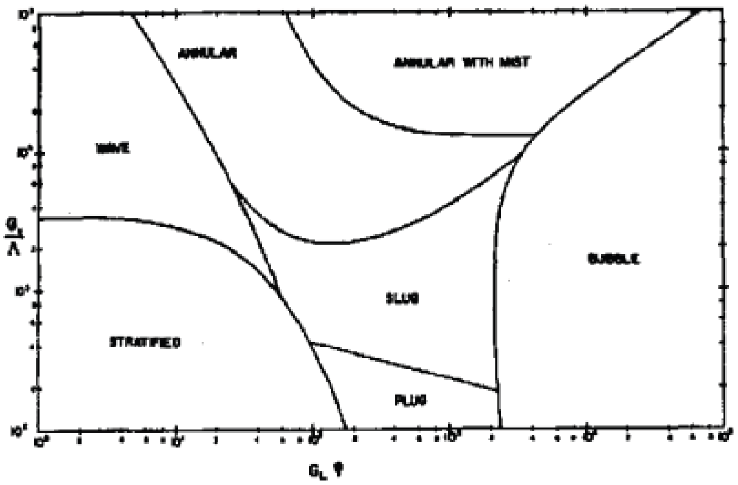

Figure 13: Baker's map for horizontal flow modified by Bell et al. (Bell et al., 1970).

And finally, this last map has been redrawn again, regaining the old dimensionless units of Baker, and changing the units of the map to SI units. The result is in the figure 14, and this is the map which is in the website application, the "Modified Baker's map for horizontal tube".

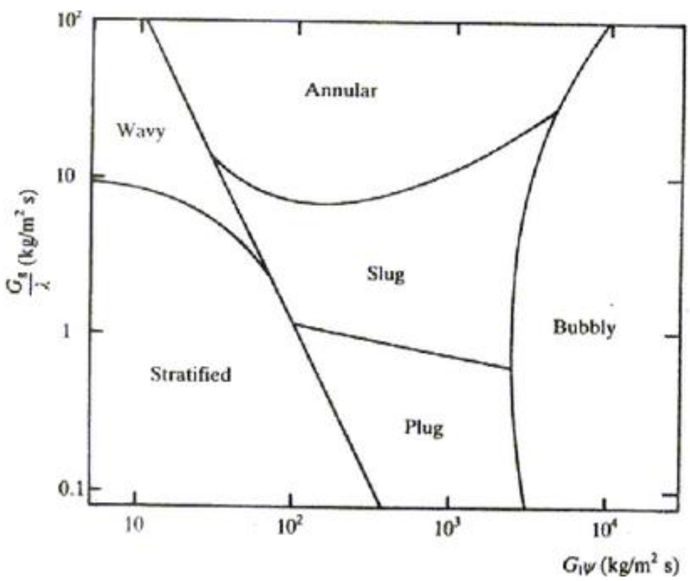

Figure 14: Modified Baker's map for horizontal flow (Whalley, 1987).

The axes are given by a kind of combination of Bell's and Baker's coordinates:

X-axis: $G_L\psi$ [kg/m² s]

Y-axis: $\frac{G_v}{\lambda}$ [kg/m² s]

Where λ and ψ are the dimensionless Baker's parameters defined in equations 19 and 20.

8.2 Properties of the experiment. Limitations of the map

Baker's map was made with the data of Jenkins (Jenkins, 1947), Gazley (Gazley, 1949), Alves (Alves, 1953) and Kosterin (Kosterin, 1949), so he does not specify any experimental conditions on his paper. Furthermore, the map has two different versions, one including the data from Hoogendoorn (Hoogendoorn, 1959) and Govier and Omer (Govier and Omer, 1964), so we should take this data into account as well. However, we can say, generally, that the map is reasonably good for water/air and oil/gas mixtures in small diameter (< 0.05 m) pipes.

The map was developed using 1, 2 and 4-inch diameter pipe and air/water mixtures near atmospheric pressures at a temperature of 68 degrees F:

*Properties of the pipe:

-Diameter: 2.54 – 10.160 cm

*Pressure: 0 – 1 barg

*Liquid density: 1000 kg/m³

*Liquid viscosity: $1 \cdot 10^{-3}$ kg/m s

*Surface tension: $73 \cdot 10^{-3}$ kg/s²

*Temperature: 20 °C

9. Conclusions and recommendations

After analyzing the maps, there are some indications that can be useful. We have two kinds of maps: the experimental maps and the theoretical maps. The experimental maps are restricted by the conditions of the experiment, so one should use the one which is closer to the purpose of the researcher. However, there are some contradictions between the different maps with similar experimental conditions. It could be due to the difficulty of distinguish the pattern by visual way, or to the lack of experimental points. Anyway, there are some maps which show better results than others, and we have made a list with them. On the other hand, we have the theoretical maps, which are not restricted to experimental conditions, but assume some ideal behaviors. Most of these maps have been tested with some experiments, and they seem to have even better results than the experimental ones, but one cannot prove their good behavior in very different conditions. Nevertheless, since this kind of map is working in some specific conditions for which the map not was particularly created, one can assume that the theoretical assumes are good, and is more reliable way to extrapolate to other different conditions than the experimental ones.

Summing up, it is better to use a theoretical map, but we also can choose one of the experimental. In that case, one has to be careful with the specific conditions of his experiment.

Now, we name the most useful two-phase flow maps. The experimental conditions are specified in their sections (we also add the Barnea map and Taitel up-flow vertical map, which are not explained in the document):

Type of flow	map	year
Vertical down-flow	Barnea Unified model (**Theoretical**)	1987
	Oshinowo – Charles's map for down-flow	1974
	Golan & Stenning's map	1970
Vertical up-flow	Oshinowo – Charles's map for up-flow	1974
	Taitel and Dukler's map (**Theoretical**)	1980
	Barnea Unified model (**Theoretical**)	1987
	Hewitt and Roberts's map for vertical tubes outflow	1969
Horizontal	Taitel and Dukler's map (**Theoretical**)	1976
	Barnea Unified model (**Theoretical**)	1987
	Mandhane, Gregory and Aziz map for horizontal flow	1973

10. References

[1] Alves, George E., *Co-Current Liquid-Gas Flow in a Pipeline. Contactor.* Paper presented at San Francisco meeting of A.I.Ch.E., Sept. 14, 1953.

[2] M. M. Awad, *Two-Phase Flow* (Ph. D. Thesis), Mechanical Power Engineering Department, Faculty of Engineering, Mansoura University, Egypt, 2012.

[3] Baker, O., 1954, *Simultaneous Flow of Oil and Gas*, Oil and Gas Journal, 53, pp.185-195.

[4] Bell, K. J., Taborek, J., and Fenoglio, F*. Interpretation of horizontal in-tube condensation heat transfer correlations with a two-phase flow regime map*. Chem. Eng. Prog. Symp. Ser., 66:150–163, 1970.

[5] Gazley, C., *Intertacial Shear and Stability in Two-Phase Flow*, PhD theses, Univ. Del., Newark (1949).

[6] Ghiaasiaan, S. Mostafa. *Two-phase flow, boiling, and condensation: in conventional and miniature systems.* Cambridge University Press, 2008.

[7] Golan, L.P. and Stenning, A.H. 1969*, Two-Phase Vertical Flow Maps*, Proc. Inst. Mech. Eng. Vol. 184 (3C), pp. 110-116.

[8] Govier, G. W., and Cmer, M. M., Can. I. Chem. Eng. 49, 93 (1962).

[9] Griffith, P. et al. *Slug flow*. Cambridge, Mass.: Division of Sponsored Research, Massachusetts Institute of Technology, 1959.

[10] G. F. Hewitt and D. N. Roberts, *Studies of Two-Phase Flow Patterns by Simultaneous Flash and XRay Photography*, AERE-M2159. (1969).

[11] Hoogendoorn, C. J., Chem. Eng. Sci. 9, 205 (1959).

[12] Jenkins, Rodman, *Two-Phase Two-Component Flow of Air and Water*, M.S. Thesis, University of Delaware, (1947).

[13] Kosterin, S.I., *An Investigation of the Influence of the Diameter and Inclination of a Tube on the Hydraulic Resistance and Flow Structure of Gas-Liquid Mixtures*, Izvest. Akad. Nauk. SSSR, Otdel Tekh Nauk, No. 12, (1949).

[14] Lockhart, R. W., and R. C. Martinelli, Chem. Eng. Progn, 45, No. 1, 39-43 (1949).

[15] Mandhane, J.M., Gregory, G.A., and Aziz, K., 1974. *A flow pattern map for gas-liquid flow in horizontal pipes*. International Journal of Multiphase Flow 1, 537-553.

[16] Oshinowo, T.; *Charles, M. E. Vertical two-phase flow .1. Flow pattern correlations*. Canadian Journal of Chemical Engineering, v. 52, n. 1, p. 25-35, 1974 1974. ISSN 0008-4034.

[17] Pickering, P. F., et al. *The prediction of flows in production risers-truth & myth*. *IIR Conference*. Vol. 10. 2001.

[18] Scott, D. S., 1964, *Properties of Co-Current Gas-Liquid Flow*, Advances in Chemical Engineering, 4, pp. 199-277.

[19] Shell Company, 2007. *Manual: gas/liquid separators-type selection and design rules.*

[20] Taitel, Y. and Dukler, A. E. *A model of predicting flow regime transitions in horizontal and near horizontal gas-liquid flow*. AIChE J., 22:47–55, 1976b.

[21] Whalley, P. B. *Boiling, condensation, and gas-liquid flow.* Oxford Oxfordshire. New York: Clarendon Press; Oxford University Press, 1987. xi, 291 p. ISBN 0198561814.